Journal of
Micro/Nanolithography,
MEMS, and MOEMS

SPIEDigitalLibrary.org/jm3

High-stroke, high-order MEMS deformable mirrors

Bautista R. Fernández
Mohamed Amine Bouchti
Joel Kubby

SPIE

High-stroke, high-order MEMS deformable mirrors

Bautista R. Fernández
Mohamed Amine Bouchti
Joel Kubby
University of California
Department of Electrical Engineering
MS: SOE2, 1156 High Street
Santa Cruz, California 95064
E-mail: jkubby@soe.ucsc.edu

Abstract. Monolithic fabrication of continuous facesheet high-aspect ratio gold microelectromechanical systems (MEMS) deformable mirrors (DMs) onto a thermally matched ceramic–glass substrate (WMS-15) has been performed. The monolithic process allows thick layer deposition (tens of microns) of sacrificial and structural materials thus allowing high-stroke actuation to be achieved. The fabrication process does not require wafer bonding to achieve high aspect ratio three-dimensional structures. A gold continuous facesheet mirror with 3.4 nm surface roughness has been deposited on a 16×16 array of X-beam actuators on a 1-mm pitch. A stroke of 6.4 μm was obtained when poking two neighboring actuators. Initial electrostatic actuation displacement results for a high-aspect ratio gold MEMS DM with a continuous facesheet will be discussed. © *The Authors. Published by SPIE under a Creative Commons Attribution 3.0 Unported License. Distribution or reproduction of this work in whole or in part requires full attribution of the original publication, including its DOI.* [DOI: 10.1117/1.JMM.12.3.033012]

Subject terms: adaptive optics; continuous facesheet; high-aspect ratio; MEMS; deformable mirror; electrodeposition; high stroke; high order.

Paper 13055 received Apr. 18, 2013; revised manuscript received Jun. 17, 2013; accepted for publication Jun. 21, 2013; published online Aug. 12, 2013.

1 Introduction

A monolithic fabrication process has been investigated for the development of a high-aspect ratio microelectromechanical systems (MEMS) deformable mirror (DM) for adaptive optics. Unlike current MEMS processes such as the Sandia Ultra-planar, Multilevel MEMS Technology[1] (SUMMiT) process, and the MEMSCAP PolyMUMPS[2] process that limits a DM's stroke due to the thin-film (2 μm) sacrificial layer used, the monolithic process described in this article has the ability to deposit thicker layers of structural and sacrificial materials. Thick sacrificial layer deposition will allow the DMs to provide both high-stroke and high-order corrections, thus eliminating the need for a woofer-tweeter DM configuration.[3,4]

The monolithic fabrication of the continuous facesheet DM was performed on an optically flat glass–ceramic substrates (WMS-15) that is used to make wavelength division multiplexing filters in the telecommunication industry.[5] The substrates have a root mean square roughness of <1 nm and a coefficient of thermal expansion (CTE) of 11.4×10^{-6} K^{-1} that is closely matched to the CTE of gold, 14.2×10^{-6} K^{-1}. Figure 1 shows a picture of the fabricated 6-in. wafer. The fabricated 6-in. wafer consists of sixteen 16×16 array DMs, sixteen 10×10 array DMs, sixty-four 3×3 DMs, numerous alignment structures, test structures, and layer thickness structures.

The fabrication process starts with a deposition, patterning, and lift-off of a 0.5-μm counter-electrode layer on to the glass–ceramic substrate. The actuator anchors are then patterned and electroplated to a height of 22 μm. The copper sacrificial layer is then electroplated and both the sacrificial copper and gold anchor posts are planarized with a chemical mechanical polishing (CMP) method down to a height of ~20 μm. A 4-μm gold spring layer is then patterned and electroplated followed by copper electroplating up to the height of the spring layer. The top surfaces of these layers are then planarized with CMP.

After planarization of the spring layer, 30-μm mirror support posts are patterned and electroplated. Another layer of sacrificial copper is electroplated up to the top of the post and both the copper and support posts are planarized. A final 2-μm gold mirror layer is then patterned, electroplated, and planarized to an optically flat surface. Chemical etching of the copper sacrificial layer is carried out, leaving behind a continuous facesheet attached to an array of X-beam actuators.

Figure 2 shows the general overview of the monolithic fabrication process. The X-beam actuators were designed to help prevent premature pull-in associated with unsupported actuator corners or edges, while at the same time allowing large displacements to be achieved. The actuators consist of square 400×400 μm membranes supported diagonally at the corners by four 390×20 μm fixed-guided beams.[5,6] When the actuators are displaced by more than half the thickness of the spring layer, they become nonlinear. This in turn allows mechanical "strain stiffening" to increase the travel range.[7] The actuator can be described by a nonlinear spring equation near pull-in:

$$F_m = k\delta^3, \qquad \text{(Nonlinear spring equation)} \qquad (1)$$

where δ is the actuator displacement, k is the nonlinear component of the spring constant.[8]

The relationship between the voltage and displacement for the X-beam actuator is:

$$V = [3k\delta^2(g - \delta)^3/(\varepsilon_0 A)]^{1/2}, \qquad \text{(Voltage)} \qquad (2)$$

where g is the initial actuator gap, $\delta = (3/5)g$ is the pull-in displacement, ε_0 is the dielectric constant, and A is the actuator area. The pull-in voltage is found by substituting $\delta = (3/5)g$ into Eq. 2 leading to $V_{pi} = [216\,kg^5/3125\,\varepsilon_0 A]^{1/2}$.

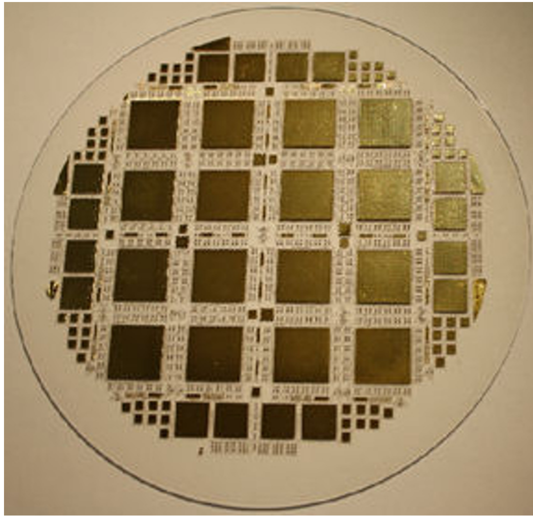

Fig. 1 Various size MEMS deformable mirrors fabricated on a 6-in. WMS-15 wafer.

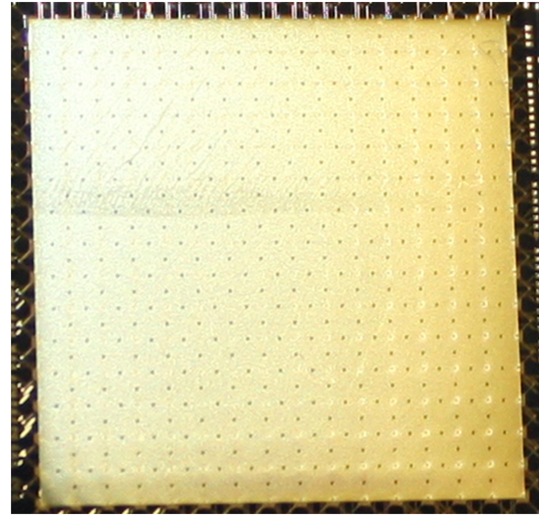

Fig. 3 Top view of the facesheet deposited on an array of 16×16 actuators on a 1-mm pitch.

2 DM Characterization

2.1 *Surface Roughness*

Previous fabrication runs suffered from layer thickness variations, stiction, and not fully released mirror arrays. Stiction is due to meniscus forces that arise during drying after wet etching. To ensure the devices were released, the wafers were placed in an etching solution for 24 h and they were pulled out several times for testing. During this process, some of the solution dried causing stiction of the actuator arrays and leaving behind stains on the mirror surface. The liquid trapped between the substrate and the actuator produced capillary forces.[9,10] These capillary forces caused the actuators to stick to the underlying substrate.[11]

In the latest fabrication run, the 6-in. wafer was diced and the 16×16 dies were individually placed in an etching solution for 24 h. Unlike the previous attempt, only one die was released at a time and was removed from the solution only once and dried using critical point drying to prevent stiction by providing a clean and dry surface. With critical point drying, a liquid to solid interface is never formed, so there is no capillary force to cause stiction.[10] This release step allowed a facesheet with an improved surface figure to be achieved. The RMS surface roughness was measured with Veeko's NT1100 interferometer to be ~3.4 nm. Figure 3 shows the top view of the fabricated facesheet.

2.2 *DM Packaging and Printed Circuit Test Board*

Six 16×16 DM die were packaged onto a 181-pin, gold-plated through-hole ceramic pin grid array (CPGA) (CPG18023, Spectrum Semiconductor Material, Inc, San Jose, California). The central 12×12 actuators (144 bonds + ground) were wire bonded to the CPGA. The outer two rows of the DM are used as spring supports for the continuous facesheet. For this particular packaging, the DMs were not hermetically sealed. A glass lid was attached to protect the mirrors from dust.

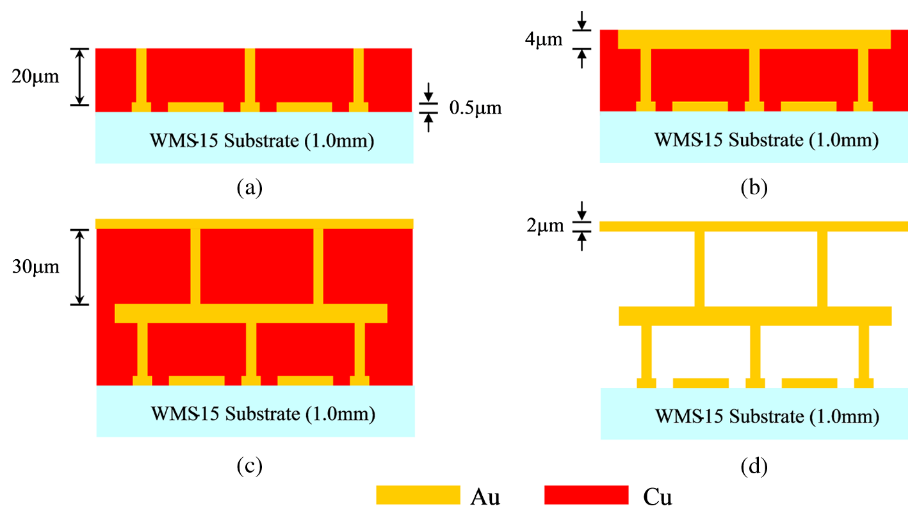

Fig. 2 Overview of the monolithic fabrication process. (a) Patterning, electroplating, and CMP of the counter electrodes and anchor posts. (b) The spring layer. (c) The mirror support posts and the mirror layer. (d) Released continuous facesheet mirror attached to actuators.

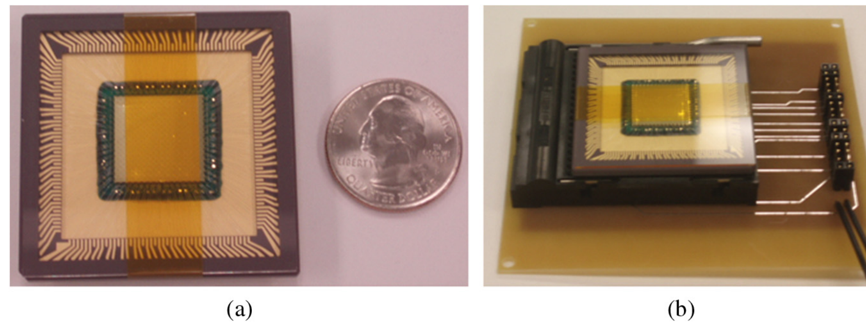

Fig. 4 (a) Top view of the packaged 16×16 array DM. (b) Assembled DM on a PCB test board.

The central 4×4 actuators of two DMs were utilized for individual and multi-actuator displacement testing. In order to perform the displacement testing, a printed circuit board (PCB) was designed and fabricated. The PCB allowed the actuation of up to 16 actuators with a single power supply by manually placing a jumper that connected the corresponding actuator's counter electrode to a power supply pin. The DM's continuous facesheet is connected to the power supply's ground. The packaged DM was placed on a ZIF PGA test and burn-in socket (181-PRS 18041-12, Aries Electronics, Inc, Bristol, Pennsylvania) allowing the DMs to be easily swapped for testing.

Figure 4(a) shows the top view of a 16×16 channel packaged DM, and Fig. 4(b) shows the assembled DM and test board.

2.3 *Single and Dual Actuator Testing*

The testing of single actuators was performed on the packaged DMs. The central 4×4 actuators of the DMs were individually tested. Figures 5 and 6 show the displacement versus voltage of two actuators individually tested with a corresponding displacement of ∼5.1 μm (actuator 1) and ∼4.6 μm (actuator 2) at 380 V, respectively. The displacement difference between actuators is due to nonuniform layer thicknesses related to CMP of the copper layer that partially attacks the gold layers. As the CMP chemistry is improved, the thickness variations within the wafer are expected to be minimized.

Figures 5 and 6 also show that the displacement versus voltage for the individual actuators is repeatable.

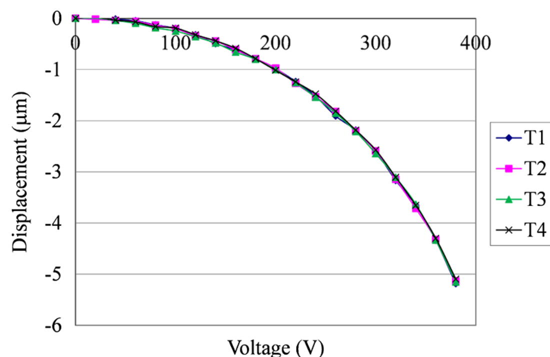

Fig. 5 Displacement versus voltage result of single poke actuator on a 16×16 DM with a maximum stroke of 5.1 μm for four test trials, $T1$ to $T4$.

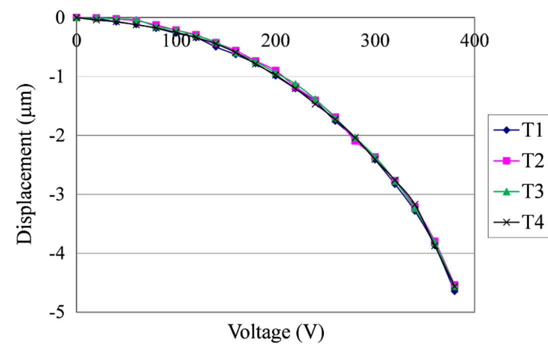

Fig. 6 Displacement versus voltage result of single poke actuator on a 16×16 DM with a maximum stroke of 4.6 μm for four test trials, $T1$ to $T4$.

Both of the above actuators were tested simultaneously at the same voltage. Figure 7 shows that actuator 1 was displaced to ∼6.4 μm and actuator 2 was displaced to ∼5.7 μm at 380 V, respectively. The voltage was not increased beyond 380 V to prevent the actuators from pull-in failure.

The DMs were tested to see if their surfaces would return to their original positions after a single actuator was displaced by ∼5.0 μm and held there for 2 min. After 2 min, the voltage was set to zero and the surface height was measured. The process was repeated 10 times on separate actuators. The test showed that the mirrors returned to their original positions with a standard deviation ranging from 0.01 to 0.05 μm for the tested actuators.

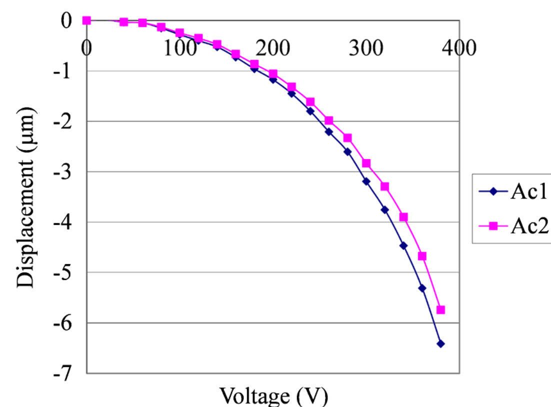

Fig. 7 Displacement versus voltage of two poked actuators tested simultaneously.

3 Future Steps

The testing of the DMs utilized the central 4×4 area of the actuators. The tested actuators were actuated by manually placing a jumper that connected the corresponding actuator's counter electrode to a power supply pin. The PCB allowed multiple actuators to be tested simultaneously by using a corresponding number of jumpers. Although the test PCB allowed the DMs to be characterized for multi-actuator displacement, all the tested actuators share the same voltage. The next step in testing the mirrors would require a larger actuator test area. A new PCB design is planned that will allow the integration of a commercial DM power supply to actuate the DM actuators at different voltages. The voltage output of the power supply will be summed to a constant voltage to allow a high-enough voltage (+380 V) to be applied to each actuator. The initial testing will be performed on the central 4×4 actuators and eventually expanded to the entire central 12×12 array of actuators. Future designs will also include the development of actuators with through-wafer vias and row–column addressing to replace actuator trace routing on the wafer and to minimize the number of traces on the PCB, respectively.

4 Conclusions

We have developed a high-aspect-ratio, monolithic process for fabricating a high-stroke MEMS DM. A facesheet, with a surface roughness of ~3.4 nm, was deposited (rather than bonded) on top of a 16×16 array of X-beam actuators on a 1-mm pitch. The DM dies were packaged in a CPGA and a custom PCB was designed and fabricated to perform multiactuator testing. The central 4×4 actuators of the packaged DMs were tested for multiactuator displacement. A stroke of 6.4 μm was obtained when poking two actuators.

Acknowledgments

This material is based upon work supported by the National Science Foundation under Grant No. AST-1032362.

References

1. J. J. Allen, *Micro Electro Mechanical System Design*, pp. 88–94, CRC Press, Taylor & Francis Group, Boca Raton, Florida (2005).
2. J. M. Bustillo, R. T. Howe, and R. S. Muller, "Surface micromachining for microelectromechanical systems," *Proc. IEEE* **86**(8), 1552–1574 (1998).
3. K. Morzinski et al., "Stroke saturation on a MEMS deformable mirror for woofer-tweeter adaptive optics," *Opt. Express* **17**(7), 5829–5843 (2009).
4. B. Fernández and J. Kubby, "Characterization and annealing of high-stroke monolithic gold MEMS deformable mirror for adaptive optics," *Proc. SPIE* **7931**, 79310A (2011).
5. B. R. Fernández and J. Kubby, "High-aspect-ratio microelectromechanical systems deformable mirrors for adaptive optics," *J. Micro/Nanolitho. MEMS MOEMS* **9**(4), 041106 (2010).
6. B. R. Fernández, "Design, fabrication and characterization of high-stroke high-aspect ratio micro electro mechanical systems deformable mirrors for adaptive optics," Ph.D. Thesis, Univ. of California Santa Cruz, Dept. of Electrical Engineering (2011).
7. E. S. Hung and S. D. Senturia, "Extending the travel range of analog-tuned electrostatic actuators," *J. Microelectromech. Syst.* **8**(4), 497–505 (1999).
8. G. M. Rebeiz *RF MEMS: Theory, Design, and Technology*, pp. 21–58, John Wiley & Sons, Hoboken, New Jersey (2003).
9. O. Raccurt et al., "Influence of liquid surface tension on stiction of SOI MEMS," *J. Micromech. Microeng.* **14**(7), 1083–1090 (2004).
10. I. Jafri, H. Busta, and S. Walsh, "Critical point drying and cleaning for MEMS technology," *Proc. SPIE* **3880**, 51–58 (1999).
11. S. Beeby et al., *MEMS Mechanical Sensors*, Artech House, Inc., Norwood (2004).

Bautista R. Fernández obtained his PhD in electrical engineering from the University of California, Santa Cruz, with a concentration in microelectromechanical systems (MEMS) with applications in adaptive optics. He obtained a BS and MS degree in electrical engineering from the University of California, Santa Cruz, in 2004 and 2007, respectively.

Mohamed Amine Bouchti is a PhD student in electrical engineering at the University of California, Santa Cruz, with a concentration in MEMS for adaptive optics and biomedical applications. He received his BS degree in electrical engineering and computer science from the University of California, Berkeley, in 2009.

Joel Kubby is a professor and department chair of electrical engineering in the Baskin School of Engineering at the University of California at Santa Cruz. His research is in the area of MEMS with applications in Optics, Fluidics, and Bio-MEMS. Prior to joining the University of California Santa Cruz in 2005, he was a manager with the Wilson Center for Research and Technology and a member of technical staff in the Webster Research Center in Rochester New York (1987 to 2005). Prior to Xerox, he was at the Bell Telephone Laboratories in Murray Hill New Jersey working in the area of Scanning Tunneling Microscopy (STM). He has a PhD in applied physics from Cornell University and a BA in physics from the University of California Berkeley. He is the co-chair of the SPIE Silicon Photonics conference and the MEMS Adaptive Optics conference.